Supplementary Material Cover Sheet

Comparison of the enhanced roles of chemical surfactant and bio-surfactant in the adsorption of tetracycline onto iron oxides

Yang Liu [1], Kunyu Wen [1], Qiang Zhang [3], Taotao Lu [4],

Usman Farooq [2,*], Zhichong Qi [1,**]

[1] Henan Joint International Research Laboratory of Environmental Pollution Control Materials, College of Chemistry and Molecular Sciences, Henan University, Kaifeng 475004, China

[2] Miami College, Jinming Campus, Henan University, Kaifeng 475004, China

[3] Ecology institute of the Shandong academy of sciences, Qilu University of Technology (Shandong Academy of Sciences), Jinan 250353, China

[4] College of Hydraulic Science and Engineering, Yangzhou University, Yangzhou, 225009, China

Manuscript prepared for *Environmental Science: Processes & Impacts*

[*]Corresponding author: Usman Farooq (usmanfarooq@henu.edu.cn);

[**]Corresponding author: Zhichong Qi (qizhichong1984@163.com).

Number of pages: 26

Number of tables: 5

Number of figures: 13

S1. Synthesis of iron oxide minerals

Goethite was synthesized using Villalobos and Leckie's method.[S1] In brief, 500 mL of a 0.5 M $Fe(NO_3)_3 \cdot 9H_2O$ and 400 mL of 2.5 M NaOH solution were mixed. The precipitate obtained was aged in an oven for 60 h at 70 °C. The resultant solid was centrifuged and washed with deionized water repeatedly until the pH was approximately 7. Then it was dried at 40 °C.

Hematite was prepared using the procedures of Bandara et al.. [S2] First, 40 g of $Fe(NO_3)_3 \cdot 9H_2O$ was dissolved in 500 mL deionized water, and 300 mL of a 1 M KOH solution and 50 mL of a 1 M $NaHCO_3$ solution were added. The pH of the solution was checked to ensure it was above 8 but below 8.5. The suspension was then aged for 5 d at 98 °C, forming a red precipitate. Excess electrolytes were removed from the final solids by vacuum filtration and rinsing with deionized water, and then dried.

S2. Adsorption studies of surfactants onto iron oxides

Adsorption studies were conducted to determine the adsorption capacity of surfactants onto iron oxides under different pH conditions. First, approximately 15 mg of iron oxides (i.e., goethite or hematite) and 20 mL of surfactant solutions (1, 3, 5, 7, or 10 mg/L) were added to each of a series of 20-mL amber glass vials. Afterwards, the vials were equilibrated for 2 days by horizontally shaking. Then, the vials were centrifuged at 8000 rpm for 20 min, and the supernatants were filtered through a 0.45 μm filtering membrane.

The concentration of rhamnolipid was determined by the chromogenic method. Rhamnolipid is a kind of glycolipid. The phenol-sulfuric acid method is the most commonly used quantitative method. [S3] That is, 2.00 mL supernatant was poured into the colorimetric tube, each of which was added with 0.05 mL 80% phenol reagent and 5 mL concentrated sulfuric acid. After full oscillation, the solution was boiled in water at 25-30℃ for 10-20 min and then cooled to room temperature. To quantify rhamnolipid, the absorbance of each concentration was measured at a wavelength of 480 nm by an ultraviolet spectrophotometer and recorded. All absorbance measurements were made using an ultraviolet-visible spectrophotometer (TU-1810PC, Purkinje General, Beijing, China).

The concentrations of SDS in the supernatants were determined using the method Purakayastha et al. used. [S4] Methylene blue (MB) is a well-known cationic dye. SDS is a methylene blue (MB) active substance and is designated as MBAS. It forms a complex with MB. After its formation, the complex was extracted into chloroform. The complex was formed between the anionic part of SDS and the cationic part of MB. The color intensity of the chloroform layer measured the SDS concentration. The maximum

absorbance values were measured at 652 nm to quantify SDS. A calibration graph was drawn in the concentration range of 0–10 mg/L of SDS concentration. A UV-vis spectrophotometer was used for all absorbance measurements.

The adsorbed surfactants were then determined by the difference between the initial and final surfactant concentrations in the aqueous phase. All experiments were run in triplicate.

Table S1. Selected properties of tetracycline.

Antibiotics	Molecular formula	Chemical structure	Molecular weight (g/mol)	Log K_{ow} [a]	pK_a	Solubility (mol/L)
tetracycline	$C_{22}H_{24}N_2O_8$	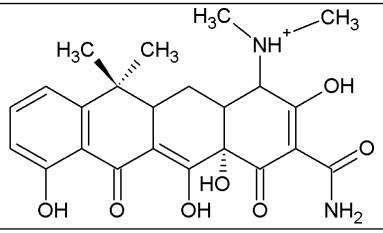	444.43	-1.30	pK_{a1}=3.32 pK_{a2}=7.78 pK_{a3}=9.58	0.041

[a] Derived from Daghrir and Drogui. [S5]

Table S2. Physical and chemical characteristics of SDS

Surfactant	Abbreviation	Molecular formula	Molecular weight	Molecular structure
Sodium dodecyl sulfate	SDS	$C_{12}H_{25}SO_4Na$	288.38	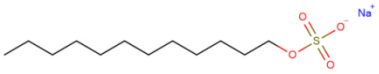

Table S3. Selected physicochemical properties of iron oxide minerals tested [a].

Iron oxide minerals	Chemical composition	*SSA* (m^2/g) [b]	pH_{PZC} [c]
Goethite	α-FeOOH	89.9	8.2
Hematite	α-Fe_2O_3	52.2	7.5

[a] derived from our previous study. [S6, S7]
[b] specific surface area;
[c] pH of zero charge.

Table S4. Sorption isotherm parameters of TC onto iron oxides under different conditions

No.	Iron oxides	antibiotic	Background solution	pH	Freundlich model				Langmuir model			
					K_F ($mg^{1-n}L^n/g$)	n	R^2	RMSE	K_L (L/mg)	q_{max} (mg/g)	R^2	RMSE
1	goethite	TC	10 mM NaCl	7.0	4.713 ± 0.122^{g}	0.492 ± 0.025^{f}	0.997	0.101	0.275 ± 0.015^{f}	18.3 ± 1.3^{g}	0.986	0.405
2	goethite	TC	10 mM NaCl + 3 mg/L Rha	7.0	5.376 ± 0.138^{f}	0.487 ± 0.027^{g}	0.991	0.163	0.332 ± 0.023^{d}	20.2 ± 0.8^{f}	0.990	0.512
3	goethite	TC	10 mM NaCl + 5 mg/L Rha	7.0	5.875 ± 0.105^{d}	0.505 ± 0.013^{d}	0.997	0.108	0.322 ± 0.012^{e}	22.8 ± 1.7^{d}	0.987	0.539
4	goethite	TC	10 mM NaCl + 10 mg/L Rha	7.0	6.199 ± 0.125^{b}	0.514 ± 0.020^{b}	0.993	0.243	0.342 ± 0.017^{c}	24.9 ± 1.2^{b}	0.983	0.716
5	goethite	TC	10 mM NaCl + 3 mg/L SDS	7.0	5.687 ± 0.100^{e}	0.507 ± 0.025^{e}	0.997	0.095	0.347 ± 0.012^{b}	21.3 ± 0.5^{e}	0.986	0.413
6	goethite	TC	10 mM NaCl + 5 mg/L SDS	7.0	6.103 ± 0.202^{c}	0.519 ± 0.013^{c}	0.994	0.117	0.356 ± 0.010^{a}	24.6 ± 1.9^{c}	0.975	0.698
7	goethite	TC	10 mM NaCl + 10 mg/L SDS	7.0	6.879 ± 0.089^{a}	0.620 ± 0.009^{a}	0.995	0.087	0.331 ± 0.013^{d}	27.8 ± 0.8^{a}	0.990	0.213
8	hematite	TC	10 mM NaCl	7.0	3.542 ± 0.027^{g}	0.567 ± 0.011^{a}	0.995	0.063	0.156 ± 0.021^{g}	14.2 ± 1.1^{g}	0.967	0.539
9	hematite	TC	10 mM NaCl + 3 mg/L Rha	7.0	3.718 ± 0.092^{f}	0.518 ± 0.025^{d}	0.998	0.057	0.176 ± 0.011^{f}	15.5 ± 1.0^{f}	0.980	0.402
10	hematite	TC	10 mM NaCl + 5 mg/L Rha	7.0	4.154 ± 0.067^{d}	0.475 ± 0.010^{f}	0.996	0.089	0.306 ± 0.019^{b}	16.7 ± 0.7^{e}	0.982	0.359
11	hematite	TC	10 mM NaCl + 10 mg/L Rha	7.0	4.546 ± 0.111^{b}	0.459 ± 0.018^{g}	0.995	0.107	0.347 ± 0.010^{a}	18.7 ± 1.5^{c}	0.973	0.378
12	hematite	TC	10 mM NaCl + 3 mg/L SDS	7.0	3.842 ± 0.107^{e}	0.513 ± 0.009^{e}	0.998	0.076	0.202 ± 0.016^{e}	17.6 ± 0.7^{d}	0.971	0.269
13	hematite	TC	10 mM NaCl + 5 mg/L SDS	7.0	4.268 ± 0.086^{c}	0.545 ± 0.023^{b}	0.996	0.089	0.211 ± 0.007^{d}	20.7 ± 1.9^{b}	0.976	0.233
14	hematite	TC	10 mM NaCl + 10 mg/L SDS	7.0	5.105 ± 0.213^{a}	0.521 ± 0.012^{c}	0.997	0.103	0.283 ± 0.018^{c}	23.4 ± 0.5^{a}	0.988	0.316
15	goethite	TC	10 mM NaCl	5.0	3.869 ± 0.129^{c}	0.524 ± 0.017^{c}	0.992	0.251	0.234 ± 0.009^{c}	15.1 ± 0.3^{c}	0.990	0.131
16	goethite	TC	10 mM NaCl + 10 mg/L Rha	5.0	5.331 ± 0.134^{b}	0.616 ± 0.022^{b}	0.993	0.206	0.254 ± 0.015^{b}	23.5 ± 1.6^{b}	0.988	0.203
17	goethite	TC	10 mM NaCl + 10 mg/L SDS	5.0	5.839 ± 0.251^{a}	0.618 ± 0.039^{a}	0.989	0.272	0.337 ± 0.022^{a}	25.9 ± 1.5^{a}	0.970	0.355
18	hematite	TC	10 mM NaCl	5.0	2.539 ± 0.035^{c}	0.375 ± 0.023^{c}	0.992	0.269	0.411 ± 0.019^{a}	10.5 ± 1.0^{c}	0.956	0.498
19	hematite	TC	10 mM NaCl + 10 mg/L Rha	5.0	3.347 ± 0.042^{b}	0.536 ± 0.036^{b}	0.997	0.079	0.174 ± 0.025^{c}	17.2 ± 1.8^{b}	0.988	0.269
20	hematite	TC	10 mM NaCl + 10 mg/L SDS	5.0	4.346 ± 0.031^{a}	0.554 ± 0.017^{a}	0.998	0.061	0.204 ± 0.020^{b}	22.3 ± 1.7^{a}	0.981	0.257
21	goethite	TC	10 mM NaCl	9.0	3.072 ± 0.052^{c}	0.606 ± 0.010^{b}	0.992	0.176	0.135 ± 0.016^{b}	16.8 ± 0.7^{c}	0.985	0.209
22	goethite	TC	10 mM NaCl + 10 mg/L Rha	9.0	3.801 ± 0.038^{b}	0.598 ± 0.029^{c}	0.997	0.063	0.135 ± 0.016^{b}	20.7 ± 1.2^{b}	0.991	0.103
23	goethite	TC	10 mM NaCl + 10 mg/L SDS	9.0	4.251 ± 0.089^{a}	0.634 ± 0.021^{a}	0.997	0.059	0.140 ± 0.016^{a}	22.9 ± 0.8^{a}	0.989	0.225
24	hematite	TC	10 mM NaCl	9.0	2.001 ± 0.105^{c}	0.625 ± 0.028^{c}	0.998	0.043	0.096 ± 0.008^{b}	12.3 ± 0.5^{c}	0.989	0.179
25	hematite	TC	10 mM NaCl + 10 mg/L Rha	9.0	2.135 ± 0.113^{b}	0.671 ± 0.015^{a}	0.996	0.156	0.081 ± 0.013^{c}	14.1 ± 1.1^{b}	0.992	0.181
26	hematite	TC	10 mM NaCl + 10 mg/L SDS	9.0	2.265 ± 0.077a	0.645 ± 0.031^{b}	0.995	0.139	0.099 ± 0.012^{a}	15.8 ± 0.9^{a}	0.990	0.227

The different lowercase letters indicate a significant difference among the different surfactant concentrations under a specified pH condition ($p < 0.05$).

Table S5. Adsorption amount of surfactants onto iron oxides (15 mg) under different solution chemistry conditions. Error bars represent standard deviations from replicate experiments (n=3)

No.	Iron oxide	ionic strength	pH	Concentration of surfactant	*q* (mg-surfactant/g-mineral)
1	goethite	10 mM NaCl	7.0	3 mg/L Rha	0.83 ± 0.02^{f}
2	goethite	10 mM NaCl	7.0	5 mg/L Rha	1.09 ± 0.05^{e}
3	goethite	10 mM NaCl	7.0	10 mg/L Rha	1.86 ± 0.07^{b}
4	goethite	10 mM NaCl	7.0	3 mg/L SDS	1.22 ± 0.03^{d}
5	goethite	10 mM NaCl	7.0	5 mg/L SDS	1.65 ± 0.08^{c}
6	goethite	10 mM NaCl	7.0	10 mg/L SDS	2.31 ± 0.06^{a}
7	hematite	10 mM NaCl	7.0	3 mg/L Rha	0.52 ± 0.03^{f}
8	hematite	10 mM NaCl	7.0	5 mg/L Rha	0.87 ± 0.11^{e}
9	hematite	10 mM NaCl	7.0	10 mg/L Rha	1.54 ± 0.05^{b}
10	hematite	10 mM NaCl	7.0	3 mg/L SDS	0.95 ± 0.06^{d}
11	hematite	10 mM NaCl	7.0	5 mg/L SDS	1.23 ± 0.15^{c}
12	hematite	10 mM NaCl	7.0	10 mg/L SDS	1.88 ± 0.11^{a}
13	goethite	10 mM NaCl	5.0	10 mg/L Rha	2.69 ± 0.15^{b}
14	goethite	10 mM NaCl	5.0	10 mg/L SDS	3.05 ± 0.07^{a}
15	hematite	10 mM NaCl	5.0	10 mg/L Rha	1.87 ± 0.07^{b}
16	hematite	10 mM NaCl	5.0	10 mg/L SDS	2.37 ± 0.16^{a}
17	goethite	10 mM NaCl	9.0	10 mg/L Rha	1.06 ± 0.03^{b}
18	goethite	10 mM NaCl	9.0	10 mg/L SDS	1.75 ± 0.12^{a}
19	hematite	10 mM NaCl	9.0	10 mg/L Rha	0.87 ± 0.05^{b}
20	hematite	10 mM NaCl	9.0	10 mg/L SDS	1.36 ± 0.10^{a}

The different lowercase letters indicate a significant difference among the different surfactant concentrations under a specified pH condition ($p < 0.05$).

(a)

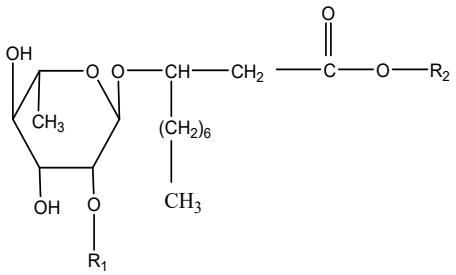

(b)

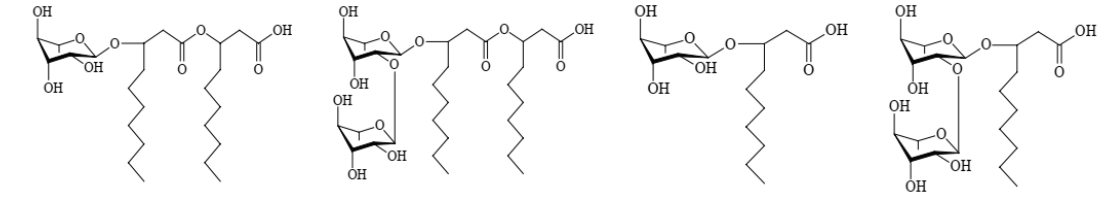

RL-1($RhC_{10}C_{10}$) RL-2($Rh_2C_{10}C_{10}$) RL-3(RhC_{10}) RL-4(Rh_2C_{10})

Fig. S1. Chemical structure of rhamnolipid with general formula; [S8] and (b) four common rhamnoolipid structures. Typically, RL-1($RhC_{10}C_{10}$) and RL-2($Rh_2C_{10}C_{10}$) were considered to be the main rhamnolipidic congeners, having variable relative proportions in mixture (RL respents rhamnoolipid). [S9]

(a) XRD

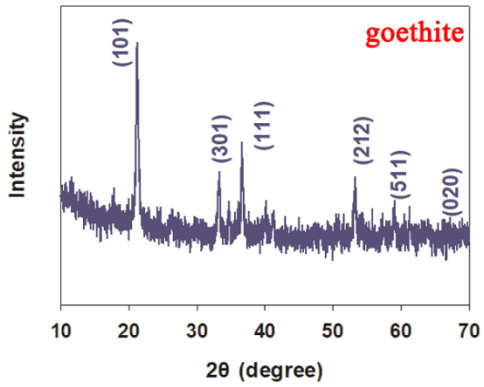

(b) XRD

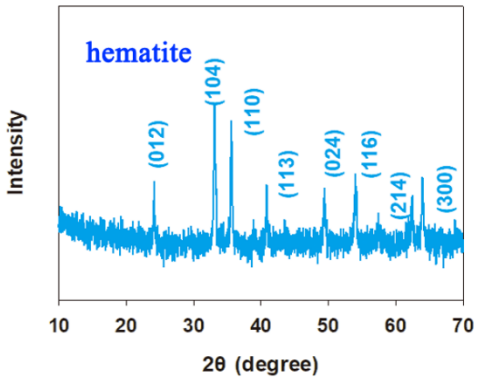

(c) SEM

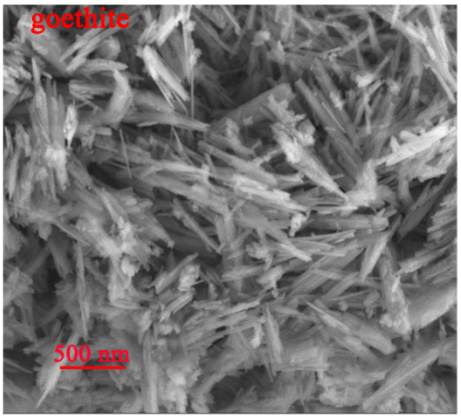

(d) SEM

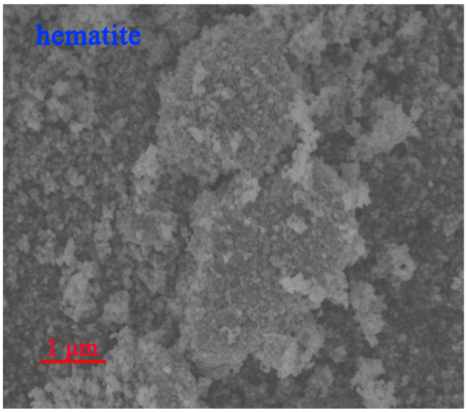

(e) FTIR

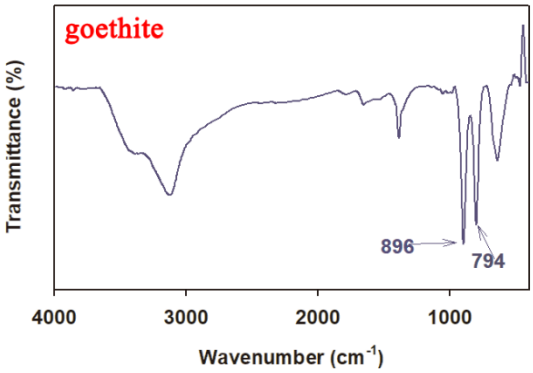

(f) FTIR

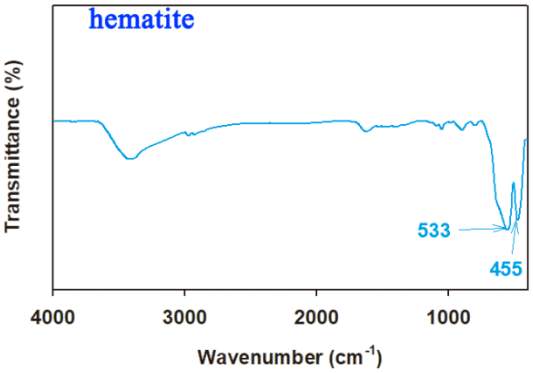

Fig. S2. Characteristics of iron oxides: (a) and (b) X-Ray Diffraction (XRD); (c) and (d) representative scanning electron microscope (SEM) images; and (e) and (f) FTIR. The peaks at 896 cm^{-1} and 794 cm^{-1} could be assigned to the Fe–OH in goethite; [S10] the peaks at 533 cm^{-1} and 455 cm^{-1} could be assigned to the Fe–OH in hematite. [S11]

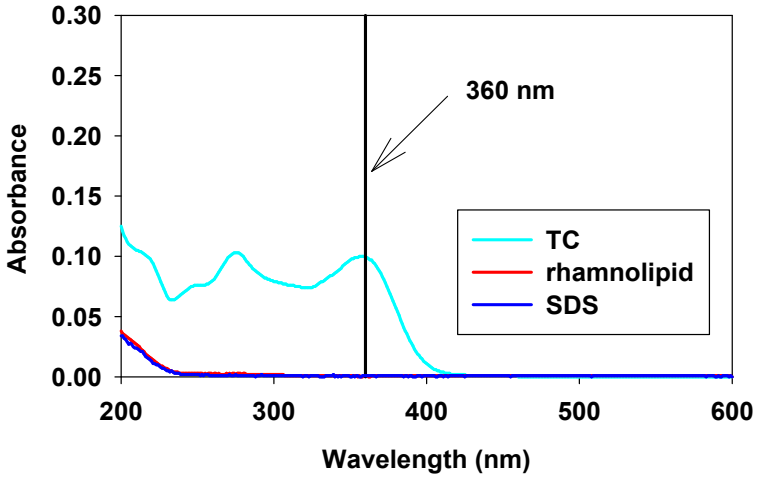

Fig. S3. (a) UV/Vis spectra of the TC solution (10 mg/L) and surfactants (10 mg/L) dispersed in DI water.

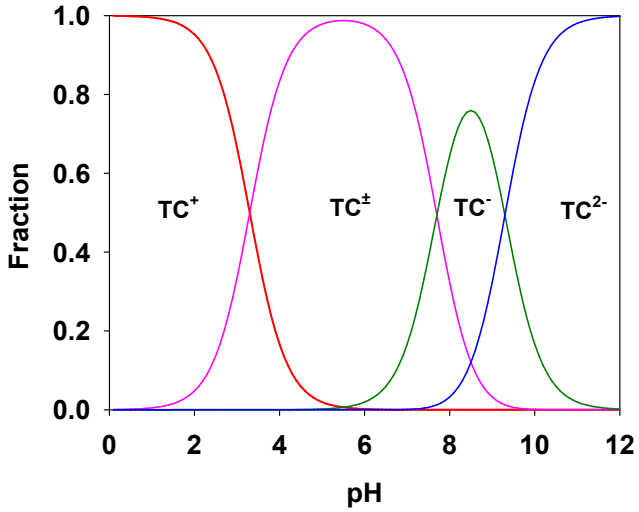

Fig. S4. pH-dependent speciation of the whole TC molecular.

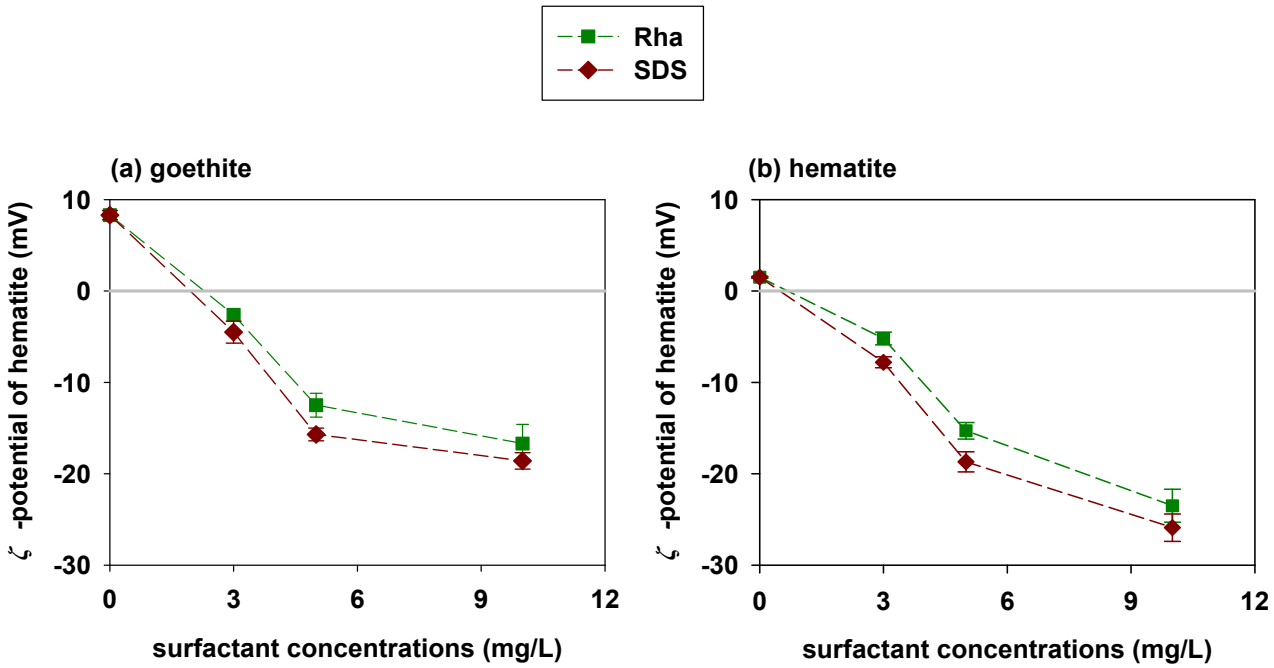

Fig. S5. Effects of surfactants on the zeta potential of (a) goethite and (b) hematite at pH 7.0.

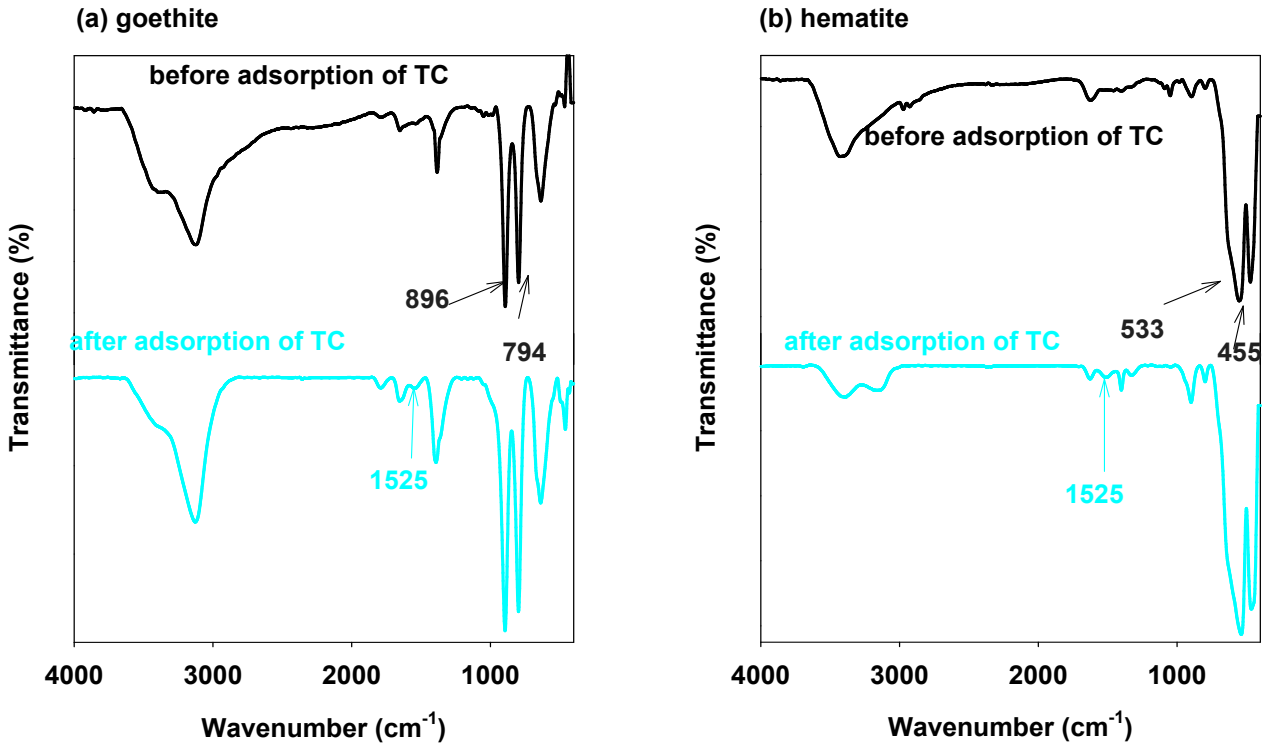

Fig. S6. Fourier transform infrared (FTIR) spectra of (a) goethite and (b) hematite before and after TC adsorption. The apparent characteristic bands (1525 cm^{-1}) of ferrihydrite after adsorption of TC were the amino C–N in the amide group of TC. [S12]

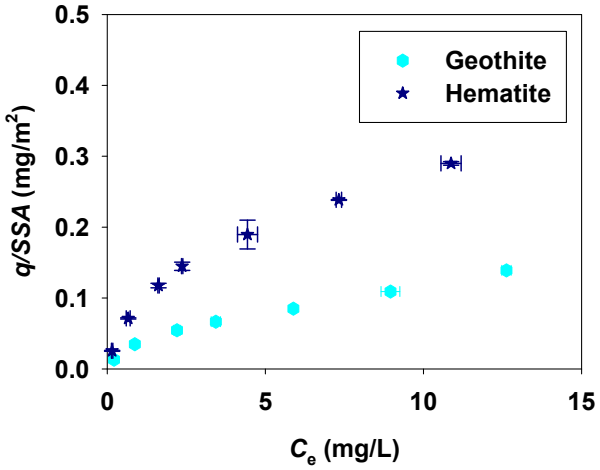

Fig. S7. *SSA* normalized adsorption isotherms of TC onto iron oxides. C_e (mg/L) is the equilibrium aqueous concentration of antibiotics; *q/SSA* (mg/m^2) is the concentration of antibiotic molecules per the specific surface area for the iron oxides.

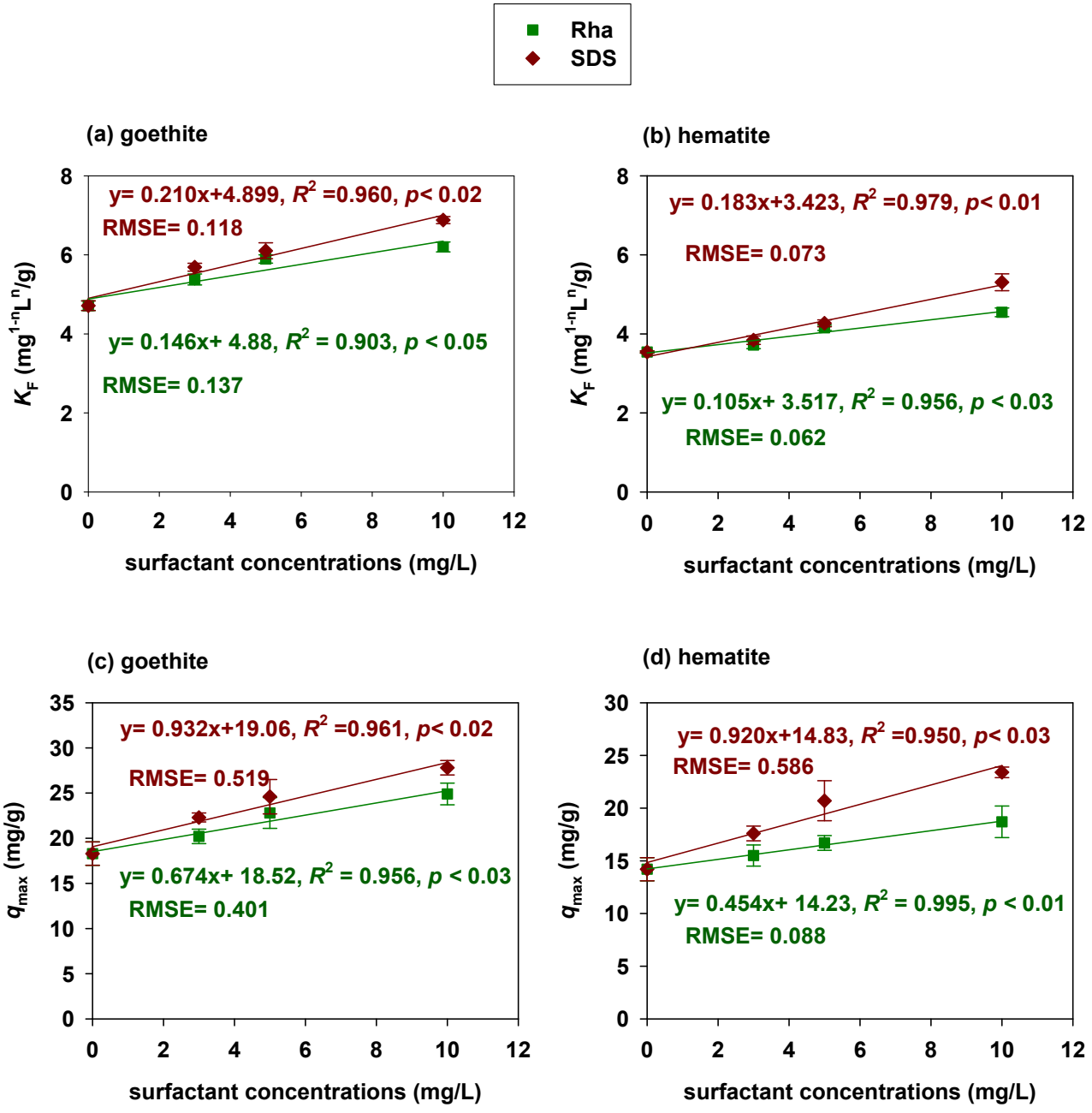

Fig. S8. (a) and (b) Comparison between the Freundlich adsorptive capacity (K_F) and concentrations of surfactants; (c) and (d) Comparison between the theoretical maximum adsorption capacity (q_{max}) and concentrations of surfactants.

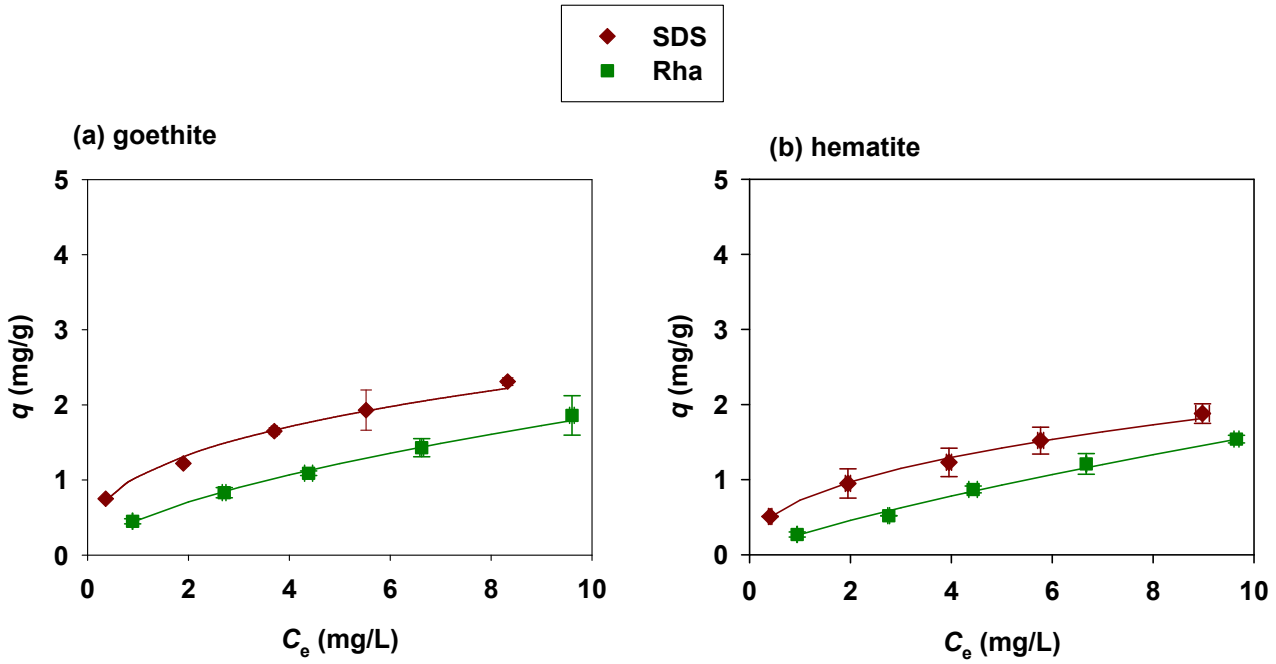

Fig. S9. Adsorption of surfactants onto iron oxides: (a) goethite and (b) hematite. pH = 7.0, $m_{minerals}$ (initial) = 15 mg, and ionic strength = 10 mM NaCl. The solid lines on the panel are the Freundlich model fitting results. Error bars represent standard deviations of triplicate samples (each with $p < 0.05$).

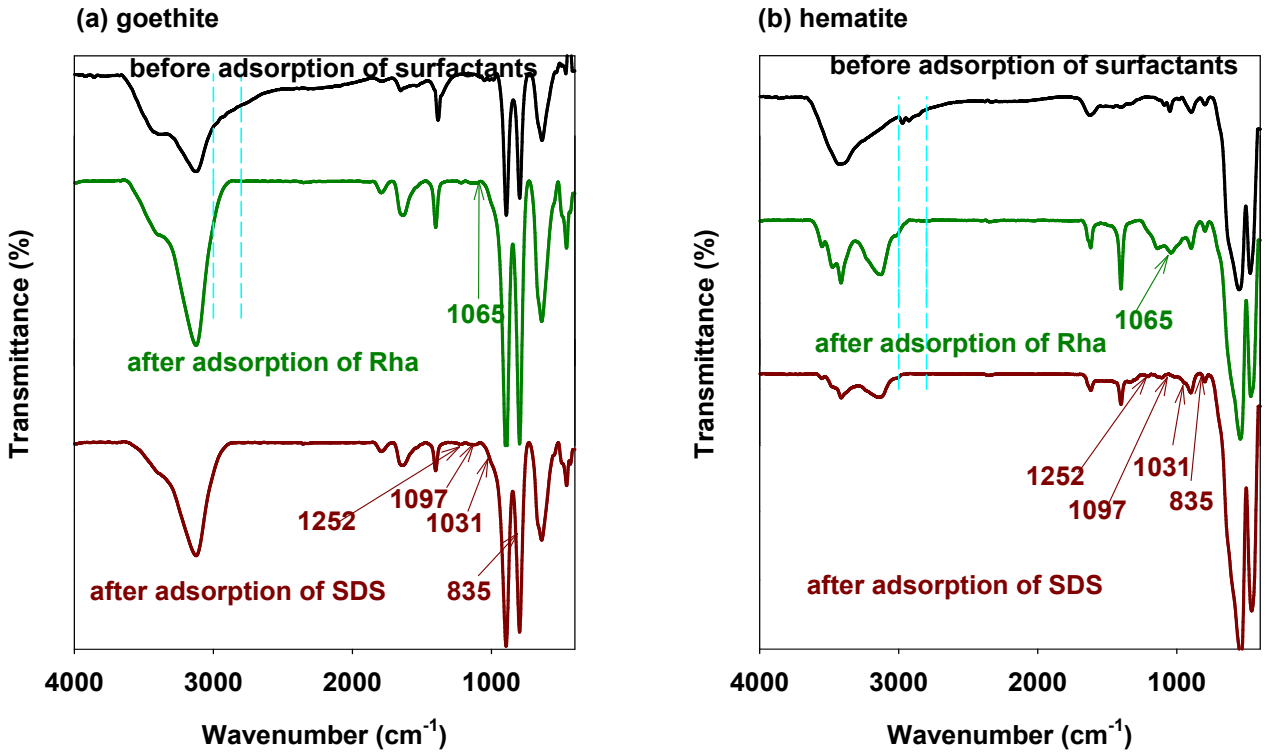

Fig. S10. Fourier transform infrared (FTIR) spectra of (a) goethite and (b) hematite before and after adsorption of Rha or SDS. For Rha, the region at the 3000−2800 cm cm^{-1} contained the asymmetric stretching vibration and stretching vibration of $-CH_2$. S13 The identified peaks around1065 cm^{-1} represent hydroxy ester bond (C–O). [S14] For SDS, the absorption band assigned to S=O symmetrical stretching vibration appears at 1097 cm^{-1} and for sulfate groups asymmetric stretching vibration appears at 1252 cm^{-1}. [S15, S16] Two bands, at 835 cm^{-1} and 1031 cm^{-1}, belong to the stretching vibration of S−O bond. [S16]

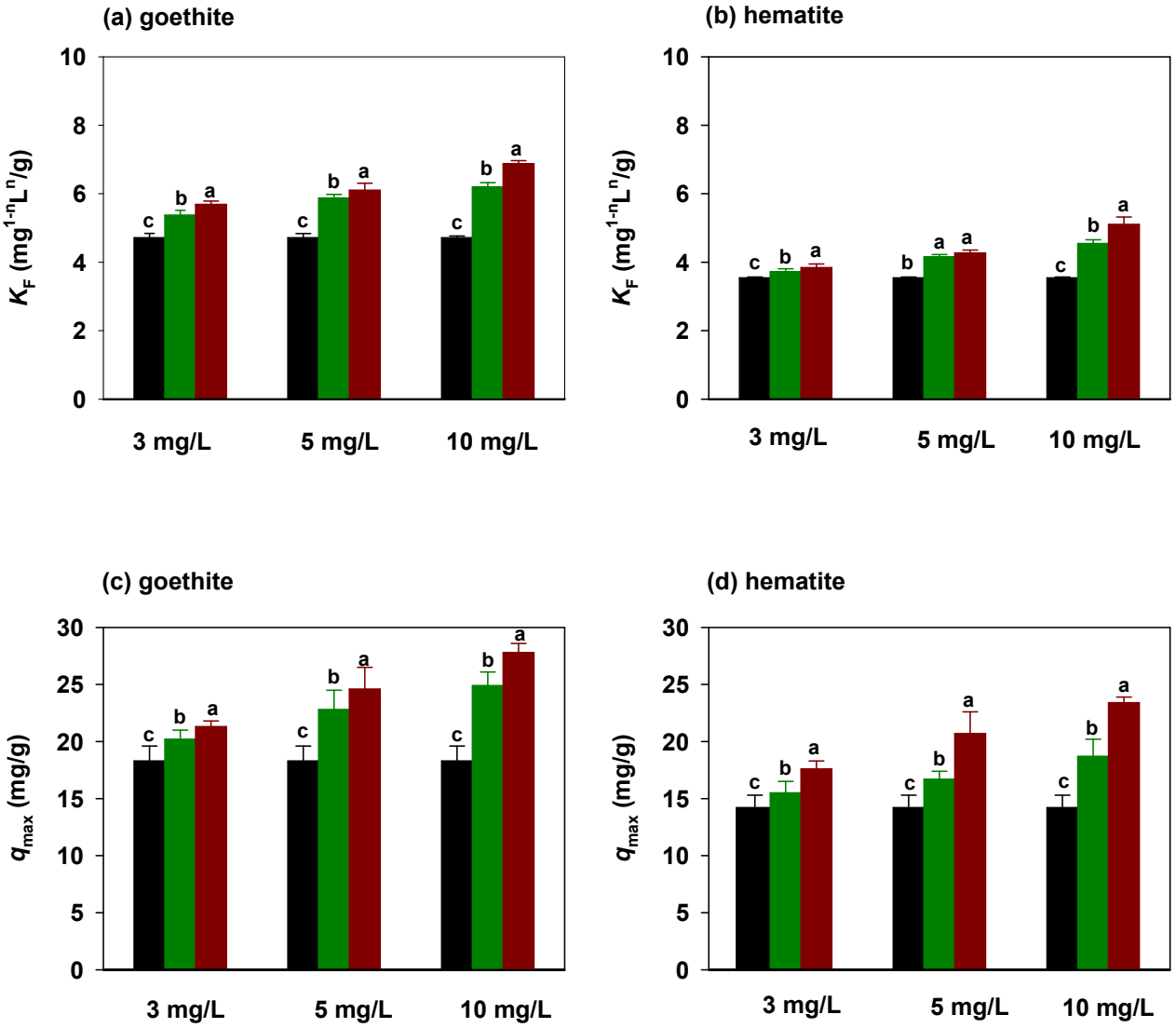

Fig. S11. (a) and (b) Effects of surfactants on the Freundlich affinity coefficient (K_F) of different iron oxides for TC under different surfactant concentration conditions; (c) and (d) Effects of surfactants on the theoretical maximum adsorption capacity (q_{max}) of different iron oxides for TC under different surfactant concentration conditions. The different lowercase letters indicate a significant difference among different surfactant additions for a given surfactant concentration ($p < 0.05$).

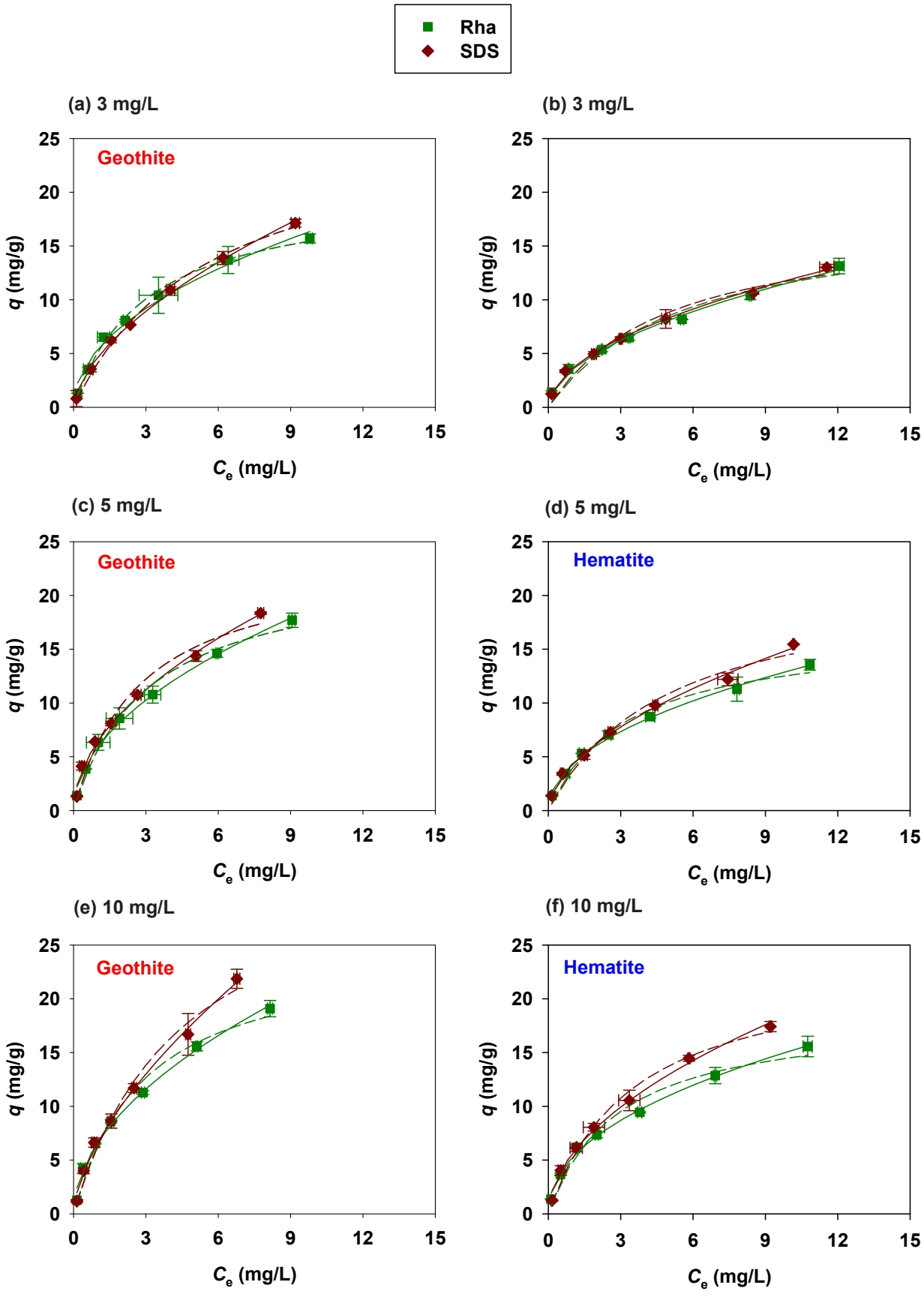
Rha
SDS
(a) 3 mg/L
Geothite
(b) 3 mg/L
(c) 5 mg/L
Geothite
(d) 5 mg/L
Hematite
(e) 10 mg/L
Geothite
(f) 10 mg/L
Hematite
q (mg/g)
Ce (mg/L)
0
5
10
15
20
25
0
3
6
9
12
15

Fig. S12. Adsorption behaviors of TC onto iron oxides in the presence of different surfactants: (a), (c), and (e) adsorption of TC onto goethite; (b), (d), and (f) adsorption of TC onto hematite. C_e (mg/L) is the equilibrium aqueous concentration of TC; q (mg/g) is the concentration of TC adsorbed on iron oxides. pH = 7.0, $m_{minerals}$ (initial) = 15 mg, and ionic strength = 10 mM NaCl. The solid lines and dotted lines on the panel are the Freundlich and Langmuir model fitting results, respectively.

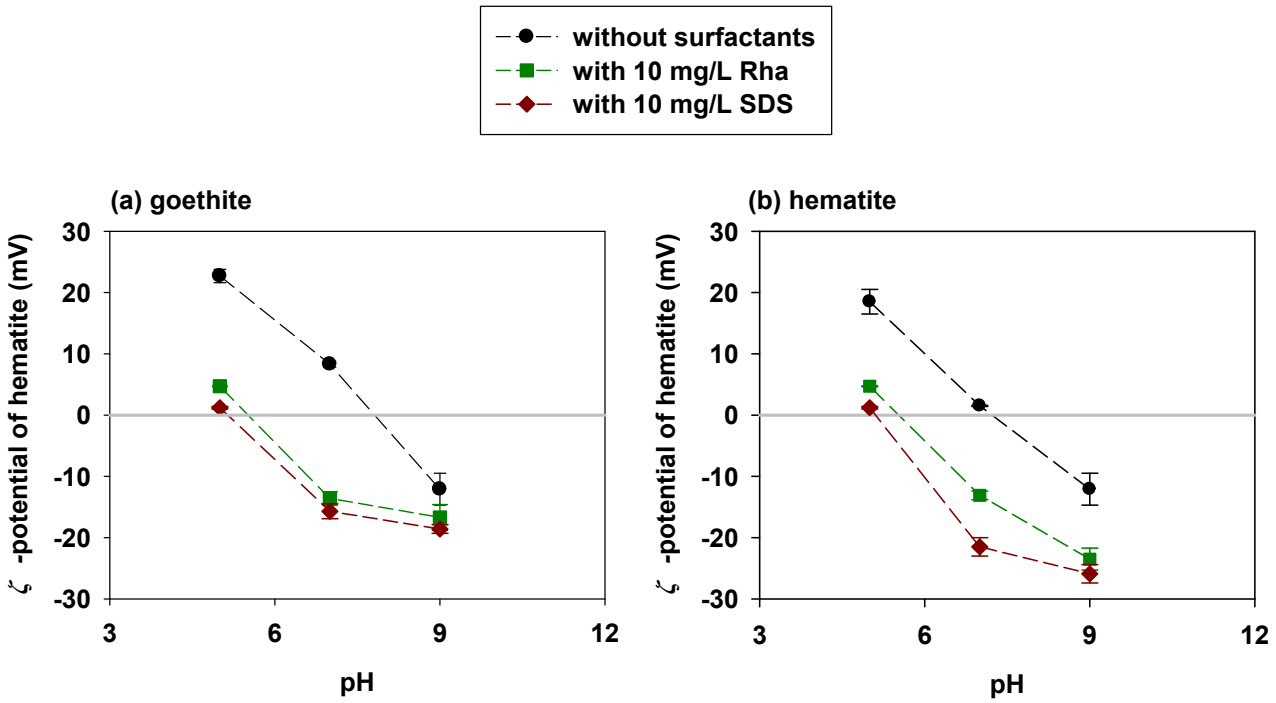

Fig. S13. The zeta potential of (a) goethite and (b) hematite in the absence or presence of 10 mg/L surfactants as affected by different pH.

References

S1. M. Villalobos and J.O. Leckie, Surface complexation modeling and FTIR study of carbonate adsorption to goethite, *J. Colloid Interface Sci.*, 2001, **235**, 15–32.

S2 J. Bandara, K. Tennakone and J. Kiwi, Surface mechanism of molecular recognition between aminophenols and iron oxide surfaces, *Langmuir*, 2001, **17**, 3964–3969.

S3. J. Jiang, M. Jin, X. Li, Q. Meng, J. Niu and X.W. Long, Recent progress and trends in the analysis and identification of rhamnolipids, *Appl. Microbiol. Biot.*, 2020, **104**, 8171–8186.

S4. P. das Purakayastha, A. and Pal, M. Bandyopadhyay, Adsorption of anionic surfactant by a low-cost adsorbent, *J. Environ. Sci. Health, Part A*, 2002, **37**, 925–938.

S5. R. Daghrir and P. Drogui, Tetracycline antibiotics in the environment: a review, *Environ. Chem. Lett.*, 2013, **11**, 209–227.

S6. M. Wang, T. Lu, W. Chen, H. Zhang, W. Qi, M. Song and Z. Qi, Enhanced role of humic acid on the transport of iron oxide colloids in saturated porous media under various solution chemistry conditions. *Colloid Surf. A.*, 2020, **607**, 125486.

S7. Y. Zhu, Q. Yang, T. Lu, W. Qi, H. Zhang, M. Wang, Z. Qi and W. Chen, Effect of phosphate on the adsorption of antibiotics onto iron oxide minerals: Comparison between tetracycline and ciprofloxacin, *Ecotox. Environ. Saf.*, 2020, **205**, 111345.

S8. T.T. Nguyen and D.A. Sabatini, Characterization and emulsification properties of rhamnolipid and sophorolipid biosurfactants and their applications. *Int. J. Mol. Sci.*, 2011, **12**, 1232–1244.

S9. Y.P. Guo, Y.Y. Hu, R.R. Gu and H. Lin, Characterization and micellization of rhamnolipidic fractions and crude extracts produced by Pseudomonas aeruginosa mutant MIG-N146. *J. Colloid Interface Sci.*, 2009, **331**, 356–363.

S10. X. Song and J.F. Boily, Water vapor adsorption on goethite, *Environ. Sci. Technol.*, 2013, **47**, 7171–7177.

S11. H. D. Ruan, R.L. Frost and J.T. Kloprogge, The behavior of hydroxyl units of synthetic goethite and its dehydroxylated product hematite, *Spectrochim. Acta A*, 2001, **57**, 2575–2586.

S12. C. Gu and K.G. Karthikeyan, Interaction of tetracycline with aluminum and iron hydrous oxides, *Environ. Sci. Technol.*, 2005, **39**, 2660–2667.

S13. L. Sang, G. Wang, L. Liu, H. Bian, L. Jiang, H. Wang, Y. Zhang, W. Zhang, C. Peng and X. Wang, Immobilization of Ni (II) at three levels of contaminated soil by rhamnolipids modified nano zero valent iron (RL@nZVI): Effects and mechanisms, *Chemosphere*, 2021, **276**, 130139.

S14. B. Muthukumar, R. Duraimurugan, P. Parthipan, R. Rajamohan, R. Rajagopal, J. Narenkumar, A. Rajasekar and T. Malik, Synthesis and characterization of iron oxide nanoparticles from Lawsonia inermis and its effect on the biodegradation of crude oil hydrocarbon, *Sci. Rep.*, 2024, **14**, 11335.

S15. A. Iovescu, G. Stîngă, M. E. Maxim, M. Gosecka, T. Basinska, S. Slomkowski, D. Angelescu, S. Petrescu, N. Stănică, A. Băran and D. F. Anghel, Chitosan-polyglycidol complexes to coating iron oxide particles for dye adsorption, *Carbohyd. Polym.*, 2020, **246**, 116571.

S16. M. Shalbafan, F. Esmaeilzadeh and G. R. Vakili-Nezhaad, Enhanced oil recovery by wettability alteration using iron oxide nanoparticles covered with PVP or SDS, *Colloids Surf. A*, 2020, **607**, 125509.